Immunobiology 222 (2017) 1053–1063

Contents lists available at ScienceDirect

Immunobiology

journal homepage: www.elsevier.com/locate/imbio

HTLV-1-infected thymic epithelial cells convey the virus to CD4$^+$ T lymphocytes

Luciana Rodrigues Carvalho Barros[a,b], Leandra Linhares-Lacerda[a,b], Klaysa Moreira-Ramos[c], Marcelo Ribeiro-Alves[d], Maria Cristina Machado Motta[e], Dumith Chequer Bou-Habib[a,b], Wilson Savino[a,b,*]

[a] Laboratory on Thymus Research, Oswaldo Cruz Institute/Oswaldo Cruz Foundation, Av. Brasil 4365, Manguinhos, 21045-900, Rio de Janeiro, RJ, Brazil
[b] National Institute of Science and Technology on Neuroimmunomodulation (INCT-NIM), Brazil
[c] Alagoas State University of Health Sciences, R Jorge de Lima, 113, 57010-382 Maceió, AL, Brazil
[d] HIV/AIDS Clinical Research Center, Evandro Chagas National Institute of Infectology/Oswaldo Cruz Foundation, Av. Brasil 4365, Manguinhos, 21045-900, Rio de Janeiro, RJ, Brazil
[e] Hertha Meyer Laboratory of Cellular, Carlos Chagas Filho Institute of Biophysics, Federal University of Rio de Janeiro, R Carlos Chagas Filho, 373, 21941-590 Rio de Janeiro, RJ, Brazil

ARTICLE INFO

Keywords:
HTLV-I infection
CD4$^+$ T lymphocytes
Thymic epithelial cells
Cell migration
Neuropilin-1
Chemokines

ABSTRACT

The human T-lymphotropic virus type-1 (HTLV-1) is the causative agent of adult T cell leukemia/lymphoma (ATL) and HTLV-1 associated myelopathy/tropical spastic paraparesis (HAM/TSP). CD4$^+$T cells are the main target of HTLV-1, but other cell types are known to be infected, including immature lymphocytes. Developing T cells undergo differentiation in the thymus, through migration and interaction with the thymic microenvironment, in particular with thymic epithelial cells (TEC) the major component of this three dimensional meshwork of non-lymphoid cells. Herein, we show that TEC express the receptors for HTLV-1 and can be infected by this virus through cell–cell contact and by cell-free virus suspensions. The expression of anti-apoptosis, chemokine and adhesion molecules genes are altered in HTLV-1-infected TEC, although gene expression of antigen presentation molecules remained unchanged. Furthermore, HTLV-1-infected TEC transmitted the virus to a CD4$^+$ T cell line and to CD4$^+$ T cells from healthy donors, during *in vitro* cellular co-cultures. Altogether, our data point to the possibility that the human thymic epithelial cells play a role in the establishment and progression of HTLV-1 infection, functioning as a reservoir and transmitting the virus to maturing CD4$^+$ T lymphocytes, which in turn will cause disease in the periphery.

1. Introduction

The human T-lymphotropic virus type 1 (HTLV-1) is the etiologic agent of adult T cell leukemia (ATL) and of neurodegenerative disorder HTLV-1 associated myelopathy/tropical spastic paraparesis (HAM/TSP). In addition, a variety of other immune-mediated chronic inflammatory conditions, such as uveitis, infectious dermatitis, myasthenia gravis, have been associated with HTLV-1 infection (Taylor and Matsuoka, 2005). Only 2–5% of HTLV-1 carriers will progress to HAM/TSP or ATL forms of the disease, in general at an onset age of 35–50 years old (Starling et al., 2013). Yet, by now there is no clear evidence of which factors are responsible for the development of each of those illnesses.

HTLV-1 is a retrovirus that infects and propagates in CD4$^+$ T cells, but cell-free HTLV-1 virions are poorly infectious, being the cell-to-cell contact considered the major route of viral transmission (Hoshino, 2012). Several distinct mechanisms of HTLV-1 cell-to-cell transmission have been proposed, such as virological synapse (VS), biofilm-like extracellular viral assemblies (Pais-Correia et al., 2010) and conduit formation (Prooyen et al., 2010; Van Prooyen et al., 2010). The vs is formed at the point of contact of HTLV-1-infected T cells with uninfected target cells, through binding of viral envelop proteins with HTLV-1 cell receptors, also including the interaction between cell adhesion molecules (Van Prooyen et al., 2010). The biofilm-like structures are composed of carbohydrate-rich extracellular assemblies, which, upon cell–cell adherence, allow virus transmission to target cells (Pais-Correia et al., 2010). The HTLV-1 encoded protein 8 (p8) increases T-cell conjugation and cluster formation, thus facilitating viral transfer to

* Corresponding author at: Laboratório de Pesquisas sobre o Timo, Instituto Oswaldo Cruz/Fiocruz. Av. Brasil 4365, Manguinhos – Pav Leonidas Deane/510, 21045-900, Rio de Janeiro, RJ, Brazil.
E-mail addresses: savino@fiocruz.br, savino.w@gmail.com (W. Savino).

http://dx.doi.org/10.1016/j.imbio.2017.08.001
Received 2 February 2017; Received in revised form 1 June 2017; Accepted 9 August 2017
Available online 14 August 2017

neighbor uninfected T cells through cellular conduits[6]. It is possible that HTLV-1 uses multiple strategies to establish efficient viral transmission between cells (Franchini, 1995).

Irrespective of the contact mechanism, the initial step in HTLV-1 infection involves the polarization of HTLV-1-infected cell microtubule-organizing center (MTOC), followed by specific interactions between viral envelope proteins and the target cell receptors glucose transporter-1 (GLUT-1) (Manel et al., 2003), neuropilin-1 (NRP-1) (Ghez et al., 2006) and heparin sulfate proteoglycans (HSPGs) (Jones et al., 2005), allowing the entrance of viral particles, proteins and genomic RNA into uninfected target cells (Manel et al., 2003). Although $CD4^+$ T cells correspond to the main target of HTLV-1 infection, HTLV-1 entry receptors are largely expressed on the surface of other cells types, making them permissive to HTLV-1 infection. Indeed, there is evidence that $CD8^+$ T cells (Nagai and Osame, 2003), immature lymphocytes (Maguer-Satta et al., 1995; Maguer et al., 1993), $CD34^+$ progenitor cell (Nagai and Osame, 2003), astrocytes (Méndez et al., 1997), endothelial (Ho et al., 1984) and dendritic cells (Jones et al., 2008) can also be infected.

Thymic epithelial cells (TEC) are the major component of thymic microenvironment, influencing the lymphocyte maturation via Notch ligand expression and production of cytokines, chemokines, adhesion molecules and extracellular matrix (ECM) proteins, and by presenting self-peptides in the context of the major histocompatibility complex (MHC). Accordingly, immature lymphocytes expressing randomly rearranged T-cell receptor (TCR) undergo positive and negative selection events based on their ability to recognize self-peptide/MHC molecules complexes expressed by TEC. Most of these TEC-mediated processes modulate not only T-cell differentiation and migration patterns, but also the lymphocyte fate (Savino, 2010).

The strict quality control of developing T cells in the thymus culminates in the generation of self-tolerant, lineage committed T cells capable of performing the peripheral immunological functions in the periphery. There is evidence that the thymus can be a target organ for HTLV-1 infection, since HTLV-1 genome has been detected in thymus from patients with myasthenia gravis (Manca et al., 2002), and that immature lymphocytes are permissive to HTLV-1 infection *in vitro* (Maguer-Satta et al., 1995; Maguer et al., 1993). We have described that TEC can be infected by HTLV-1 *in vitro* following exposure to cell-free supernatant from the HTLV-1-infected T cell line C91PL (Moreira-Ramos et al., 2011). Now, we further show that TEC can also be infected by cell-to-cell virus transmission, and that HTLV-1-infected TEC promote T cell migration and convey the virus to primary and tumor T $CD4^+$ lymphocytes. Our data points to the possibility that TEC function as a HTLV-1 reservoir, able to transmit the virus to maturing lymphocytes.

2. Methods

2.1. Cell culture and HTLV-1-containing supernatants

Unless otherwise stated, all cells were cultured in RPMI (Sigma) supplemented with 10% of fetal bovine serum (FBS) (GIBCO), at 37 °C and 5% CO_2. The human TEC line (THF) was obtained from fetal thymus by an explant technique and limiting dilution cloning (Fernández et al., 1994), and kindly provided to us by Dr. Maria Luiza Toribio (Universidad Autonoma de Madrid, Madrid, Spain). The HTLV-1-infected $CD4^+$ T-cell line CIB was established from a patient with HTLV-1-associated myelopathy and maintained in culture medium supplemented with 50 units/mL of IL-2 (Sigma), except when CIB supernatants were collected for TEC infections assays. The $CD4^+$ T cell line C91/PL was obtained from a HTLV-1-infected patient with ATL (Ho et al., 1984). HTLV-1-negative supernatants were obtained from the leukemic $CD4^+$ T cell line CEM (Schachtschabel et al., 1966), which was used as HTLV-1 target cell in infection assay. Primary $CD4^+$ T lymphocytes from healthy donors were separated by cell sorting (FACS Aria II, BD Bioscience) from 10^8 human peripheral blood mononuclear cells (PBMC) obtained by density gradient centrifugation (Hystopaque, Sigma) from buffy coat preparations. Cells were labeled with anti-CD4 FITC and anti-CD3 Percp (BD Biosciences) and the double-positive cells were sorted using FACS Aria II (BD Biosciences) with 95% purity for $CD4^+$ T cells. These cells were activated with phytohemagglutinin (PHA) 5 μg/mL (Sigma-Aldrich) for 48 h before co-cultivation with TEC. The use of primary human T cells was approved by the Research Ethics Committee of the Oswaldo Cruz Foundation/Fiocruz (Rio de Janeiro, RJ, Brazil) under the number 397-07. Supernatants from CEM, CIB and C91/PL were collected from 2×10^6 cells after 72 h of culture in 5 mL medium, filtered (pore of 0.22 μm) (Merck-Millipore) and stored at −80 °C for future use.

2.2. HTLV-1 infections

TEC cultures were washed with warm PBS prior the addiction of other cells or supernatant. HTLV-1 TEC infections by cell-free virus suspensions were performed exposing TEC to $HTLV\text{-}1^+$ supernatants during 90 min at standard culture conditions. Then, the cells were washed with warm PBS and replenished with culture medium. TEC were also infected by co-culturing then with C91/PL or CIB at a 1:5 ratio in 8-wells glass Labtecks (NUNC) for 24 h. The ability of HTLV-1-infected TEC to transmit viruses was analyzed by co-culturing then with 10^5 uninfected CEM cells for 24 h, or primary $CD4^+$ T cells for 48 h in Labtecks (NUNC). All assays of HTLV-1 cell infections were confirmed by immunofluorescence, as described below. In some selected experiments, the HTLV-1-infected TEC were treated with AZT (10 μM) for 30 min before addition of the target $CD4^+$ tumor T cells (CEM), to analyze whether the HTLV-1 transmission from TEC to other cells was prevented by antiretroviral treatment.

2.3. Immunofluorescence staining

Cells were fixed in ethanol, washed and incubated with PBS/BSA 2% for 30 min, treated with anti-rabbit anti-human pan-cytokeratin antibody (DAKO) followed by the addition of goat anti-rabbit Cy5 1:400 (Molecular Probes). Anti-HTLV-1 p19 gag protein (10ug/mL, clone TP-7, mouse IgG1, Abcam) and anti-HTLV-1 gp46 env protein (10ug/mL, clone 67/5.5.13.1, mouse IgG1, Abcam) monoclonal antibodies were used to identify HTLV-1 in infected cells plus 1:400 rabbit anti-mouse Alexa Fluor 488-labeled secondary antibodies (Invitrogen). DAPI (Sigma-Aldrich) was added for nuclei observation; stained cells were mounted in Prolong Gold Antifade reagent (Life Technologies), and analyzed in fluorescence (Zeiss) or in confocal microscopy (FluoView FV10i, Olympus). Acquired images were quantified for $p19^+$ cells using the Image J software.

2.4. Transmission electron microscopy

The cells were fixed for 1 h in 2.5% glutaraldehyde and diluted in 0.1 M cacodylate buffer, pH 7.2. The samples were washed twice with the same buffer and fixed in 1% OsO4, 0.8% KFe(CN)6 and 5 mM CaCl2 diluted in 0.1 M cacodylate buffer. After fixation, the cells were washed, dehydrated in a graded series of acetone solutions and embedded in Epoxy resin. Ultrathin sections were stained with uranyl acetate and lead citrate before analysis with a Zeiss 900 transmission electron microscope.

2.5. Flow cytometry staining and analysis

TEC were removed from culture flasks using cell scrapers, treated with AB^+ human serum and labeled with specific antibodies during 30 min. Antibodies against the following molecules were used: CD3 Percp, CD4 FITC, CD11a PE, Neuropilin1 PE, HLA class I FITC, HLA class II APC, CD80 PE, (BD Biosciences) and the purified anti-GLUT-1

(ABCAM) plus goat anti-mouse IgG Alexa Fluor 488 (Molecular Probes). The acquisition was performed in FACSCanto II (BD Biosciences) and the data analyzed in FlowJo software (TreeStar). Apoptosis or necrosis was detected using Propidium Iodide (PI) (Sigma). To quantify cellular proliferation, TEC were labeled with CFSE (carboxyfluorescein succinimidyl ester, BD Biosciences) during for 72 h and then were acquired at the cytometer.

2.6. Microarray assay

For microarray experiments we used non-treated TEC, TEC treated with uninfected supernatant (TEC sCEM) and TEC treated with HTLV-1-infected supernatant (TEC sCIB or TEC sC91PL). Total RNA from TEC was extracted with TRIreagent (Sigma-Aldrich) according to the manufacturer's protocol. Total RNA concentration and quality was measured using NanoDrop (Thermo Scientific) and 2100 Bioanalyzer (Agilent Technologies), respectively. For microarray experiments we used 400 ng of total RNA of three independent samples for each condition, using two-color hybridizations with dye-swap in a 4 × 44 K Agilent Whole Human Gene Microarray (G4112F, Agilent Technologies). Labeling, hybridization and washing were performed according to the manufacturer's instructions (Agilent Technologies). Hybridized microarrays were scanned with a DNA microarray scanner (Agilent G2565BA) and intensities were extracted using the Agilent Feature Extraction software (AFE, version A.9.5.3) with standard protocols and options. The pre-processing and differential expression analysis of gene expression data were performed in the R programming environment (Ritz and Spiess, 2008) and processed using Bioconductor (http://www.bioconductor.com) (Gentleman et al., 2004) Agi4 × 44-PreProcess (López-Romero, 2011) library. Normalized data were scaled by the quantile method (R and M, 2002) and filtered to 1) maintain intensities within the dynamic range of the scanner (elimination of saturated points); and 2) retain genetic data of good quality. The library of the Bioconductor hgug4112a.db (Carlson, 2015) was used to assign the access code for the gene corresponding to each probe Agilent. Differential expression was analyzed with the Limma library (Smith, 2005) in empirical Bayesian methods (Smith, 2005). The Benjamini and Hochberg method (Benajmini and Hochberg, 1995) was used as control false discovery, in which a value of false discovery (FDR) of 0.05 was selected. Microarrays raw signal and fold-change values are available at the National Center for Biotechnology Information (NCBI) Gene Expression Omnibus (GEO) database, (GEO series accession n°.GSE73169).

2.7. Real time-quantitative PCR (PCRq)

The cells pellets were thawed in Qiazol followed by RNA extraction using miRNeasy (Qiagen). Total RNA concentration was measured in Nanodrop (Thermo Scientific), and 100 ng of RNA was used for qPCR using Express One Step Sybr GreenER Universal kit (Life Technologies), according to the manufacture instructions. The reaction was performed at StepOnePlus System (Life Technologies) in 20 µL of final volume, at 50 °C for 5 min, followed by 40 cycles at 95 °C for 1 s, 60 °C for 20 s and melting curve. The data were analyzed from triplicate reaction of each sample, by fitting four parameters sigmoid curves to Rn data using the library qPCR[41] for the R statistical package version 2.922 (Ritz and Spiess, 2008). Genes used in the normalization (*tfrc* and *rpl13*) were selected by the methods geNorm (Vandesompele et al., 2002) and NormFinder (Andersen et al., 2004). The comparison of means from normalized gene expression values between groups were performed by a nonparametric T-test with 1000 permutations (Berger, 2010). Results were represented in graphs displaying the mean ± standard error of mean of the expression levels from the test group relative to the control group. Two-tailed levels of significance ≤ 0.01, 0.05 and 0.1 were considered as "highly significant", "significant" and "suggestive", respectively. The primers sequences are: TRFC F-CCTGGCGTCGTGATTAGTG and R- TCGAGCAAGACGTTCAGTCC; RPL13 F- CGGACCGTGCGAGGTATGCT and R- AGCAGGAACCACCATCCGCT, B2M F- GATGAGTATGCCTGCCGTGT and R-TGCGGCATCTTCAAACCTCC, CCL2 F-CCGAGAGGCTGAGACTAACC and R-CATTGATTGCATCTGGCTGAG; CXCL1 F-TTGCCTCAATCCTGCATCCC and R-TTGGATTTGTCACTGTTCAGCA; CXCL3 F- AAACCGAAGTCATAGCCACAC and R- GGAAGTGTCAATGATACGCTG; ICAM1 F- TTCCTCACCGTGTACTGGAC and R- GGTAAGGTTCTTGCCCACTG; IL1A F- AAGGCGAAGAAGACTGACTC and R- GGCCATCTTGACTTCTTTGCT; IL6 F-TACCCCCAGGAGAAGATTCC and R- TTACATGTCTCCTTTCTCAGGG and IL8 F- AGCACACAAGCTTCTAGGAC and R- GCAAAACTGCACCTTCACA. For detection of HTLV-1 transcripts by RT-PCR, inventoried Taqman probes for Rex/Tax mRNA and GAPDH Taqman probe (both from ThermoFisher Scientific) were used. For the reaction, 150 ng of mRNA were used per assay, done in duplicates. Taqman One-Step RT-PCR Master Mix with pre-mixed ROX was used for the reactions. RT-PCR reaction was performed at StepOnePlus Real-Time PCR System (ThermoFisher Scientific) under the following conditions: 50 °C for 15 min, 95 °C for 20 min and 40 cycles of 95 °C 15 s, 60 °C 1 min.

2.8. Migration assay

Lymphocyte migratory activity towards to HTLV-1-infectedTEC was assessed in Transwell system in 24 well plates. Briefly, 5-µm pore size Transwell plates (Costar; Corning) were coated with 10 µg/mL fibronectin (Sigma-Aldrich) or BSA (Sigma-Aldrich) during 1 h at 37 °C, followed by 45 min blocking with 0,5% PBS/BSA. Infected or uninfected TEC (2.0×10^4/500 µL RPMI 1640) were added in the lower chambers and cultured for 48 h before the migration assay. Then, primary $CD4^+$ T cells (5×10^5) were added in the upper chambers in 100 µL of RPMI with 1% of BSA and, after 20 h of incubation in standard culture conditions, lymphocytes that migrated into lower chambers were removed and counted. The results are presented as total migration, and the specific migration was calculated by subtracting the amount of cells that moved into wells coated only with BSA.

2.9. Statistical analysis

The statistical analysis was performed in GraphPad Prism 5 Software using ANOVA, except for PCRq and microarray data.

3. Results

3.1. TEC express HTLV-1 entry receptors and can be infected by HTLV-1 through cell–cell contact

The initial step in HTLV-1 infection involves interactions between viral envelope proteins and the viral receptors GLUT-1, NRP-1 or HSPGs on target cell surface. We observed, by flow cytometry analysis, that the great majority of TEC express NRP-1 (Fig. 1A and supplementary Fig. 1) and GLUT-1 (Fig. 1B), and, more importantly, sixty percent of the cells are simultaneously positive for both receptors (Fig. 1C), meaning that TEC are readily permissive to HTLV-1 infection, as we have already reported (Moreira-Ramos et al., 2011). Thus, we next evaluated whether TEC could be infected by HTLV-1 through a direct cell contact, using the HTLV-1-infected $CD4^+$ T cell lines C91PL or CIB as a virus provider. We found a physical association between TEC and infected T cells. Most of TEC were positive for HTLV-1 gp46 (env) (Fig. 1E–F) and p19 (gag) protein 24 h after co-culture either with CIB, C91PL and MT-2 cell lines (Fig. 1G–I), while, as expected, no p19-positive TEC cells were observed in the coculture with HTLV-1 negative CEM cells (Fig. 1D). Collectively, these data show that TEC express the HTLV-1 entry receptors and are readily susceptible to HTLV-1 infection through cell–cell contact with other infected cells.

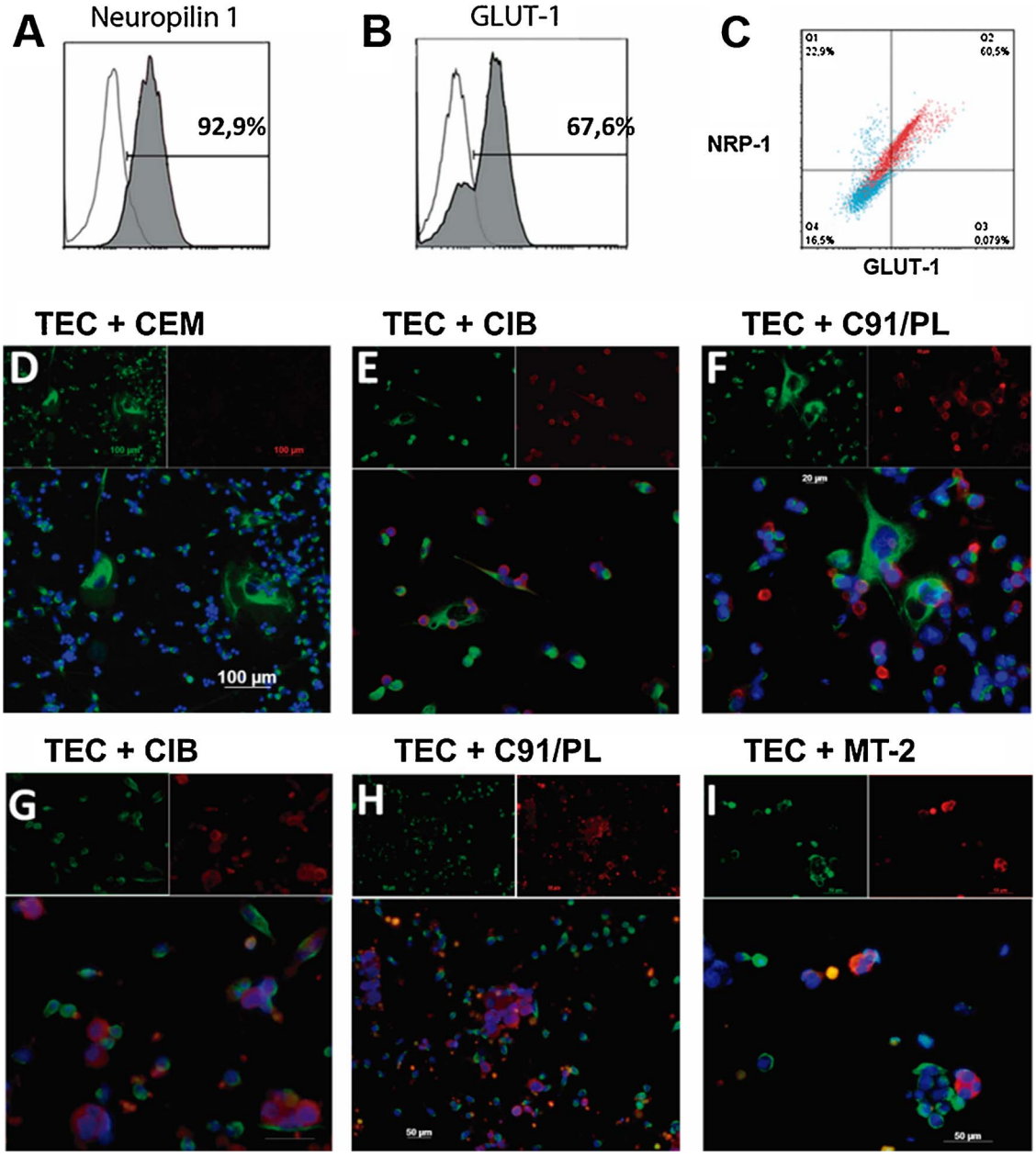

Fig. 1. TEC express HTLV-1 entry receptors and acquire HTLV-1 from chronically infected T lymphocytes by cell–cell transmission. The expression of Neuropilin-1 (NRP-1) (A) and GLUT-1 (B) was assessed by flow cytometry analysis; solid and open histograms represent the specific staining and isotype control, respectively, and are representative of tree independent experiments. A representative dot plot (C) shows the concomitant NRP-1 (red) and GLUT-1 (blue) expression in TEC. Immunofluorescence of TEC co-cultured with HTLV-1$^+$ cell lines CIB (E, G), C91/PL (F, H) and MT-2 (I). Uninfected CEM cells were used as negative control of infection (D). (D-F) Cells were stained with HTLV-1 p19 (gag) while (G-I) with gp46 (env) in red, cytokeratin in green and nuclei in blue. The small inserts above the pictures show red and green channels separately. Red: p19 or gp46. Blue: nuclei. Green: cytokeratin. (For interpretation of the references to colour in this figure legend, the reader is referred to the web version of this article.)

3.2. TEC can also be infected by cell-free HTLV-1 virions

The cell-free HTLV-1 virions have in general been considered poorly infectious, with cell-to-cell contact regarded as the main route of viral transfer *in vivo* (Matsuoka and Jeang, 2007). However, because it was described that dendritic cells were infected after exposure to cell-free HTLV-1 virions (Jones et al., 2008), we evaluated whether TEC could also be infected by HTLV-1 free particles. Thus, TEC were exposed to HTLV-1 cell-free supernatant and examined for HTLV-1 infection after different time intervals. We detected a progressive increasing number of HTLV-1-infected TEC from 24 h to 10 days after cell exposure to virus suspensions (Fig. 2A–E), indicating a massive HTLV-1 propagation in TEC culture. Indeed, quantification of infected cells demonstrated that virtually all TEC were HTLV-1$^+$ after 10 days (Fig. 2F). HTLV-1 infected TEC cultures were further analyzed by transmission electron microscopy, which shows numerous vesicles budding from infected TEC (Fig. 2G), while the uninfected TEC display a smooth membrane (Fig. 2H). On a higher magnification, vesicles containing virus particles with HTLV-1 typical structural organization were observed close to the plasma membrane, as well as the budding of a viral particle at the membrane surface (Fig. 2I) and a HTLV-1 particle that just budded from an infected TEC (Fig. 2J). The TEC infection was also confirmed by means of detecting the HTLV-1 Tax/Rex transcripts in TEC exposed to cell-free supernatant from HTLV-1$^+$ C91PL cells (Fig. 2K). The infected TEC did not present morphological alterations, death or proliferation differences, as compared with uninfected cells (Supplementary Fig. 2).

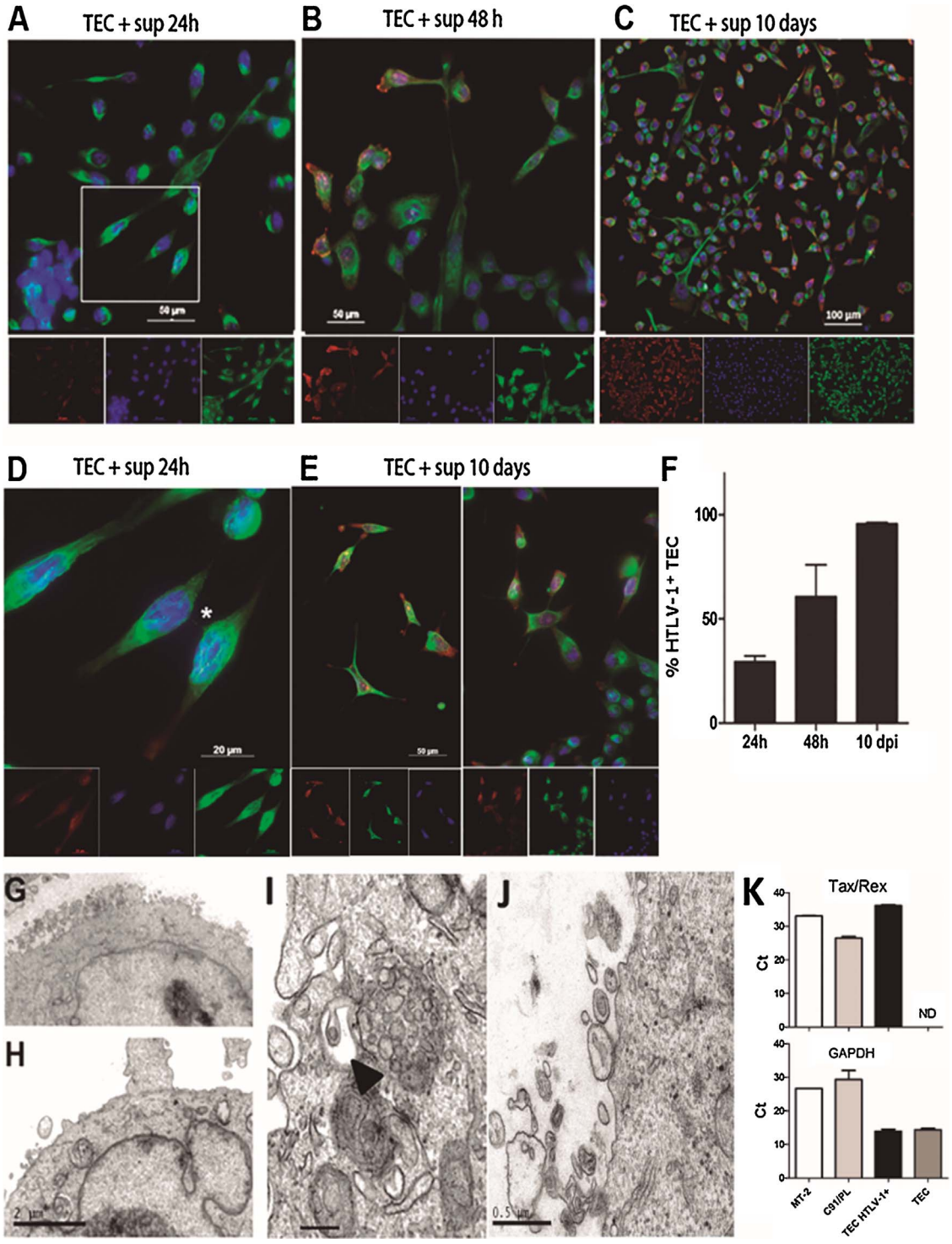

Fig. 2. TEC can be infected by cell-free HTLV-1 suspensions. TEC were treated with C91/PL supernatants during 90 min, washed, and HTLV-1 infection was evaluated by immunofluorescence after 24 h (A), 48 h (B) or 10 days (C), as indicated (TEC were labeled with cytokeratin in green, viral protein p19 in red and DAPI for nuclei in blue). (D) depicts a detail of panel A to show a (star) communication between two TEC. (E) Illustrates TEC filopodia with strong HTLV-1 labeling. The small inserts under the pictures shown each channel separately. Red: HTLV-1 p19. Blue: nuclei. Green: cytokeratin. (F) Quantification of HTLV-1$^+$TEC in different time intervals after TEC exposure to cell-free viral suspensions. Bars represent mean ± SEM from three experiments with similar results. Transmission electron microscopy of HTLV-1-infected TEC with multiple vesicles (G) and non-infected TEC (H) with a smooth membrane. A vesicle containing a virus particle (I, arrow), the budding of a viral particle from the infected cell (J, arrow). (K) HTLV-1 Tax/Rex detection by RT-qPCR in MT-2 and C91/PL cells, uninfected TEC and HTLV-1-infected TEC (ND = not detected). Bars represent amplification cycle threshold (Ct) value for three independent experiments. (For interpretation of the references to colour in this figure legend, the reader is referred to the web version of this article.)

3.3. Infected TEC maintain the expression of major histocompatibility complex

Interactions between TEC and immature lymphocytes during thymic T cell differentiation mediated by class I and class II MHC complexes and the T cell receptor (TCR) determine the fate of immature lymphocytes. Most potentially self-reactive lymphocytes are negatively selected by clonal deletion, whereas other lymphocytes are rescued

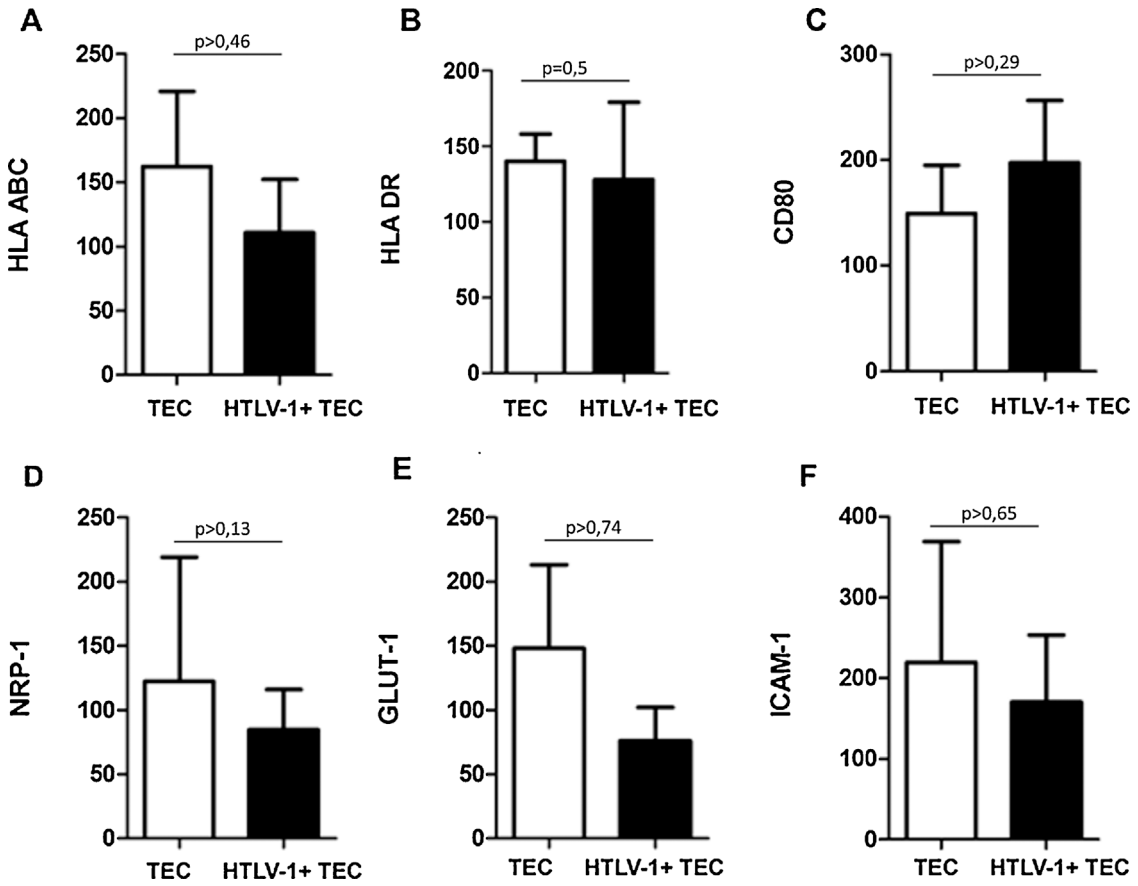

Fig. 3. HTLV-1 infection does not change TEC expression of antigen presentation, entry receptors and adhesion molecules. Uninfected and HTLV-1 infected TEC (10 days after infection), as indicated, were analyzed by flow cytometry and show similar expression of HLA class I (A), HLA class II (B), CD80 (C), NRP-1 (D), GLUT-1 (E), and ICAM-1 (F). Data present mean fluorescence intensity (MFI) and SEM from three independent experiments.

from death through positive selection, eventually yielding the vast majority of the T-cell repertoire (Savino, 2010). Because it has been described that the MHC-I surface levels are significantly decreased in human T cells expressing the p12 protein from HTLV-1 (Johnson et al., 2001), we next assessed whether the expression levels of human leukocyte antigens (HLA) and of the co-stimulatory molecule CD80 were changed in HTLV-1-infectedTEC. The expression of HLA class I (HLA-ABC) and class II (HLA-DR) molecules and CD80 was unchanged (Fig. 3A, B and C), suggesting that the antigen presentation function of HTLV-1-infected TEC to immature T cells is preserved. In addition, HTLV-1-infected TEC did not undergo a statistically significant alteration in the expression of HTLV-1 entry receptors NRP-1 and GLUT-1 (Fig. 3D and E). Importantly, infected TEC showed unaltered expression of the adhesion molecule intercellular adhesion molecule 1 (ICAM-1), which is critical in the initial formation of immunological synapses between TEC and immature lymphocytes in the thymic microenvironment (Fig. 3F).

3.4. HTLV-1 infection induces TEC chemokine gene upregulation and promotes T cell migration

Because TEC are major intrathymic chemoattractant producer, thus promoting lymphocyte migration (Savino, 2010), we next searched for gene expression modifications in HTLV-1-infected TEC, using a whole human genome microarray chip. We detected 315 differentially expressed genes, comprised by 111 upregulated and 204 downregulated relative to uninfected TEC (GEO series accession no. GSE 73169), and the gene set enrichment analysis detected 50 biological processes (Fig. 4A and Supplementary Table 1). It is worthy to highlight the enrichment of NF-κB process (Gene Ontology (GO; www.geneontology.org) (Ashburner et al., 2011), in agreement with previous findings describing NF-κB pathway activation in HTLV-1 infected cells (Currer et al., 2012). In addition, migration relevant biological process, such as taxis, leukocyte migration and regulation of chemokine production, were also enriched (Fig. 4A). Most of the migration-related genes were upregulated (Fig. 4B), and this was confirmed by real time PCR regarding the expression of CCL2, CXCL1, CXCL3 and IL-8 genes (Fig. 4C).

Because these cytokines are known to attract T lymphocytes, we evaluated the ability of HTLV-1-infected TEC to favor T cell migration, and found an increased lymphocyte movement towards HTLV-1-TEC relative to uninfected TEC (Fig. 4D), a phenomenon that corroborates the chemokine gene expression upregulation.

3.5. HTLV-1$^+$ TEC transmit virions to primary human lymphocytes

Since TEC can be infected by HTLV-1 and express adhesion molecules critical for HTLV-1 virological synapse, we next investigated whether infected TEC could transmit the virus to other HTLV-1 target cells. For this purpose, we co-cultured HTLV-1-TEC (infected by cell-free virions) with uninfected CEM cells (CD4$^+$ leukemic cell line) or with primary CD4$^+$ T cells derived from healthy donors. We found that infected TEC transmitted the virus to CEM cells (p19 positive lymphocytes), which can be seen in close contact with HTLV-1-infected TEC (Fig. 5A, top). Besides, a phylopodium structure emitted by CEM cells can be observed (Fig. 5A, bottom panels; detailed images from Fig. 5A top), which probably facilitated HTLV-1 transmission from TEC to CEM cells. Furthermore, HTLV-1-infected TEC transferred virus to primary CD4$^+$ T lymphocytes from healthy donors, as detected by HTLV-1 p19 protein-positive lymphocytes adhered to infected TEC at 48 h of co-culture (Fig. 5B–D). These figures show a massive virus transmission to

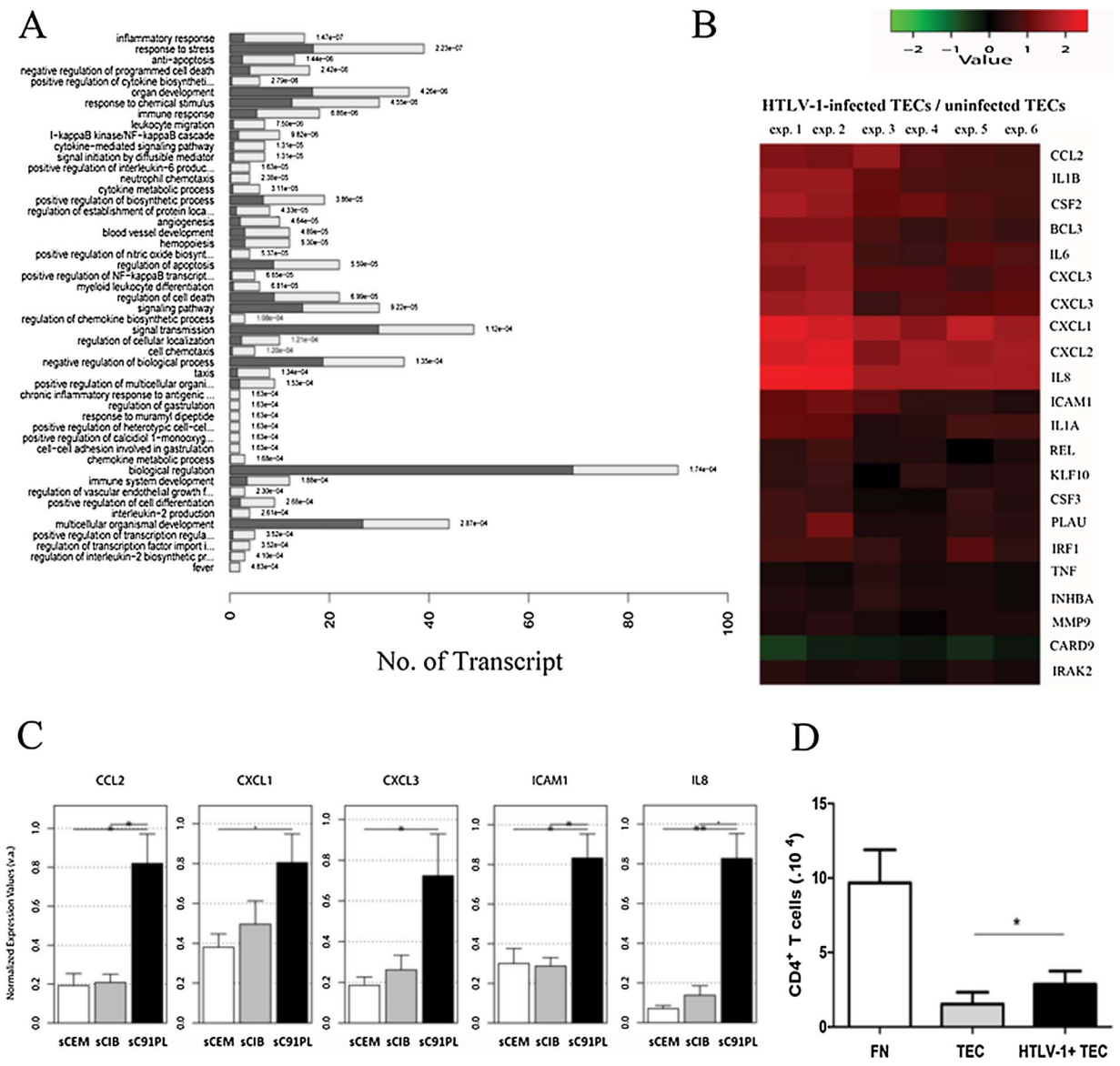

Fig. 4. HTLV-1 infection induces TEC chemokine gene upregulation and promotes T cell migration. Graphic representation of the biological process enriched based on Gene Ontology database in HTLV-1-infected TEC (A). Black bars indicates the number of expected genes differentially expressed. White bars represents the number of genes enriched in each process. Heatmap of migration-related genes (B). PCRq for CCL2, CXCL1, CXCL3 an IL8 (C). Enhanced migration of primary $CD4^+$ sorted T cells under the stimulus of HTLV-1^+ TEC (black bar) when compared to non-infected TEC (gray bar) in *transwell* chambers coated with BSA (D). Fibronectin is a positive migration control (white bar). The values shown correspond to specific migration after subtracting numbers obtained for each individual in wells coated with BSA.

T cells (Fig. 5B), multiple HTLV-1-infected lymphocytes adhered to TEC body and to phyllopodia emitted by these cells (Fig. 5C) and a confocal 3D reconstruction of HTLV-1-infected TEC and T lymphocytes (Fig. 5D). The adherence of T cells to HTLV-1-infected TEC was quantified, showing that 70% of infected TEC were specifically bound to lymphocytes (considering ≥ 3 $CD4^+$ T cells adhered to TEC as a specific attachment), suggesting that a large number of virological synapses was formed between the original and secondary infected cells (Fig. 5E). The virus transmission from TEC to T lymphocytes was dependent of a productive infection, since the co-culture treatment with the reverse transcriptase inhibitor zidovudine (AZT) decreased by 60% the virus transmission from TEC to tumor $CD4^+$ T cell line (Fig. 5F), demonstrating that an active virus replication is required for an effective virus propagation among TEC and from TEC to lymphocytes.

We next investigated whether the HTLV-1 transmission from TEC to T lymphocytes would induce fusion between those cells, triggering syncytium formation. We observed that the infection dynamics lead to induction of several different structures between both infected cells, as depicted in Fig. 6. In fact, we observed, for example, a single primary $CD4^+$ T cell engulfed by HTLV-1-infected TEC (Fig. 6A), a phylopodium emitted by $CD4^+$ T cell (Fig. 6B), a T cell spreading along and embracing the HTLV-1-infected TEC (Fig. 6C), and a TEC with multiples nuclei (Fig. 6D). Engulfment of T cells is further demonstrated in tridimensional images (Fig. 6E–G).

4. Discussion

The thymus is a primary lymphoid organ, where bone-marrow-derived T cell precursors differentiate, ultimately leading to migration of positively selected thymocytes to the peripheral lymphoid organs. The T cell development depends on interactions between developing lymphocytes and thymic epithelial cells, which influence lymphocyte maturation and migration patterns via Notch ligand expression, and production of cytokine, chemokine, adhesion molecules, extracellular matrix proteins, and by presenting self-peptides in the context of the MHC (Savino, 2010). These recent thymic lymphocyte emigrants join

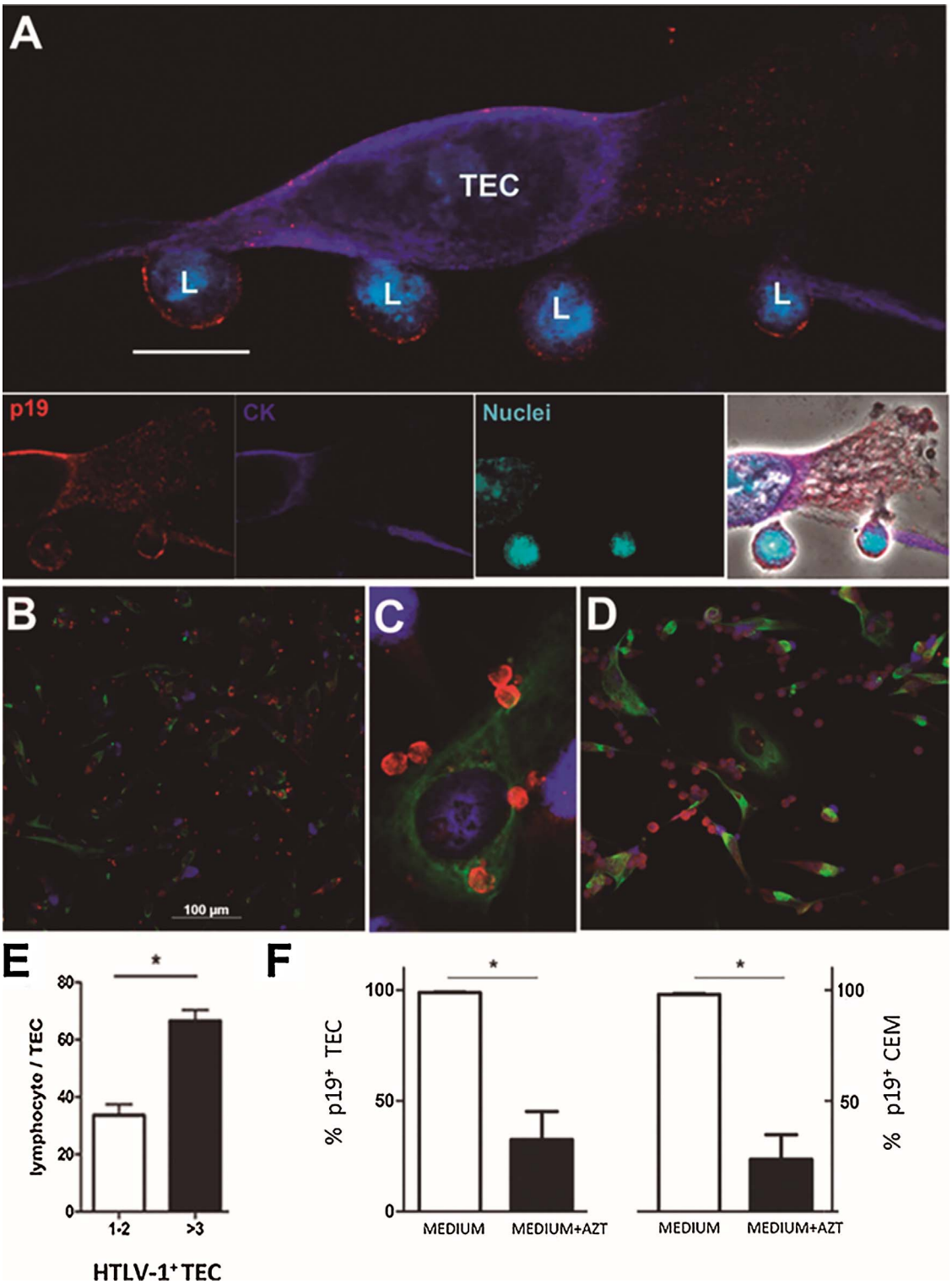

Fig. 5. HTLV-1$^+$ TEC transmit the virus to CD4$^+$ T lymphocytes. CEM cells were added to HTLV-1$^+$ TEC (A, top panel) and, after 24 h, cells were immunostained for cytokeratin (TEC, dark blue), p19 (HTLV-1, red) and nuclei (light blue; L = lymphocytes). The A bottom panels illustrate T cell phylopodia contacting infected TEC (HTLV-1 p19, red; TEC, cytokeratin dark blue; nuclei, dapi light blue, and phase contrast). Bar = 20 µm. CD4$^+$ primary T cells were added to HTLV-1$^+$ TEC (B) and, after 24 h, cells were immunostained (HTLV-1 p19, red; TEC, cytokeratin green; nuclei, dapi blue). A higher magnification of panel B is shown in C to illustrate a rosette-like formation between infected TEC and T cells. Panel D shows multiple HTLV-1$^+$ lymphocytes adhered to TEC' body and to phylopodia emitted by these cells. The number of CD4$^+$ T cells adhered to infected TEC was quantified (E), and bars represent mean ± SEM from three independent experiments. HTLV-1$^+$ TEC alone or in co-cultured with CEM cells were treated with AZT for 30 min, and the amount of p19$^+$ cells (TEC or CEM) was quantified by immunofluorescence after 48 h (F). Bars represent mean ± SEM from three independent experiments $p < 0.05$. (For interpretation of the references to colour in this figure legend, the reader is referred to the web version of this article.)

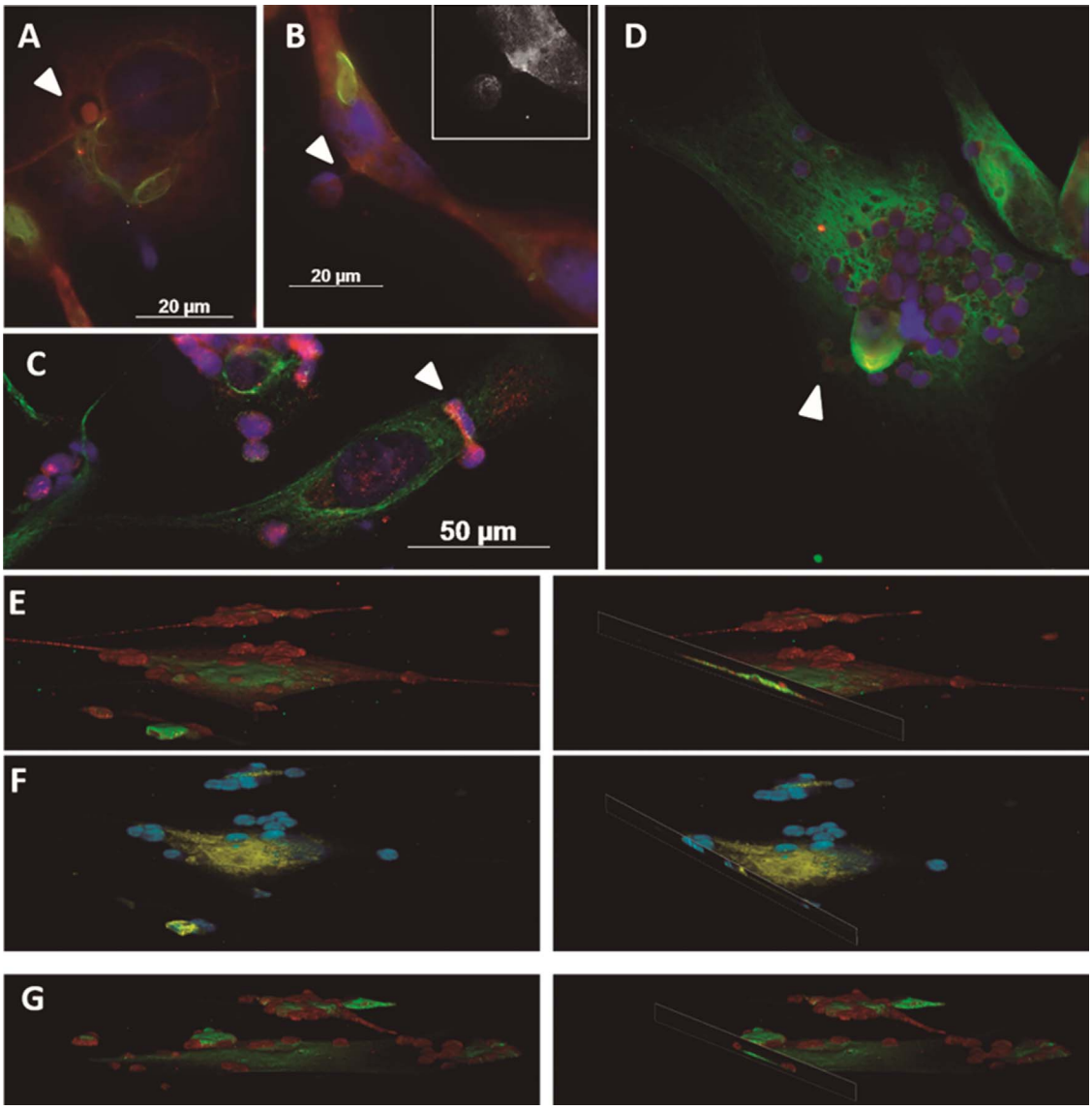

Fig. 6. HTLV-1$^+$ TEC induce different structures of CD4$^+$ T cells. Co-culture of HTLV-1 infected TEC with uninfected CD4$^+$ T cells by immunofluorescence where co-culture were labeled with cytokeratin in green, HTLV-1 viral gag protein p19 in red, and DAPI for nuclei in blue. This figure depicts a single primary CD4$^+$ T cell engulfed by HTLV-1$^+$ TEC (A, arrowhead), a phylopodium emitted by CD4$^+$ T cell (B, arrowhead), a T cell spreading along and embracing the HTLV-1$^+$ TEC (C, arrowhead), and engulfment between both infected cells TEC and T cells (D–G). Tridimensional pictures from infected cells (E–G). (For interpretation of the references to colour in this figure legend, the reader is referred to the web version of this article.)

the pool of mature peripheral T cells and can recirculate back to the thymus. Moreover, a prior exposure to antigen enhances the homing of mature T cells to the thymus (Hale and Fink, 2009). All these well-orchestrated events can be dysregulated by infections, affecting the thymus homeostasis and the T cell repertoire selection mediated by TEC (Nobrega et al., 2010). We and others have proposed that the human thymus can function as a HTLV-1 reservoir through successful infections of thymic epithelial cells (Currer et al., 2012) or thymocyte precursors (Feuer et al., 1996). This hypothesis is strengthened by the detection of HTLV-1 genome in thymuses from patients with myasthenia gravis (Manca et al., 2002). In this paper, we show new evidence that support the hypothesis that thymus stroma can be a HTLV-1 reservoir, such as the HTLV-1 propagation in TEC cultures and the ability of HTLV-1-infected TEC to transmit the virus to lymphocytes. Our present results point to the possibility that TECs can be infected in vivo by virions carried by recirculating HTLV-1-infected mature lymphocytes, or even by cell-free virus, since the HTLV-1 has been detected in the plasma of HTLV1-infected patients (Demontis et al., 2015).

TEC infection by HTLV-1 cell-free virions results in efficient and productive infection, likewise to HTLV-1-infected dendritic cells (DCs). Infected DCs maintain the expression of NRP-1 and HSPGs, two crucial molecules for efficient HTLV-1 cell binding and transferring from DCs to T cells (Jones et al., 2008). We observed that HTLV-1-infected TEC also sustain the expression of NRP-1 and GLUT-1, suggesting their involvement in virus transmission. In addition, interactions between TEC and immature lymphocytes enhance NRP-1 expression on lymphocytes (Lepelletier et al., 2007), what may favor the formation of virological synapses and may explain the high number of adhered lymphocytes per infected TEC that we saw in co-cultures. This NRP-1 enhancement may also explain the syncytium formation, since it has been demonstrated that NRP-1 increases HTLV-1 Env-mediated syncytium formation (Ghez et al., 2006). Furthermore, HTLV-1-infected TEC maintain the expression of HLA class I and class II molecules, CD80 and ICAM-1, raising the possibility of the virological synapse formation between infected TEC and lymphocytes. These findings also suggest that HTLV-1-infected TEC could present viral antigens to T lymphocytes via MHC molecules.

The HLA expression in TEC expression and the consequent self-peptides presentation are essential in lymphocyte fate decision in

thymus. In medullary TEC (mTEC), the self-peptides presentation are under the control of *Aire* (Autoimmune regulator gene), which is responsible for the expression of tissue-restricted antigen and playing a central role in the deletion of auto-reactive lymphocytes (Derbinski et al., 2001). The development of Aire$^+$ mTEC are whitin the host transcription factor NF-κB pathway, and deletion of genes involved in this pathway results in reduced Aire$^+$ mTEC (Sun et al., 2014). On other hand, it is well established that Tax, the HTLV-1 transactivator protein, interacts with and activates the NF-κB pathway, which is critical for transformation, proliferation, and survival of HTLV-1 infected cells (Currer et al., 2012). Because our expression data were obtained after only 1.5 h of infection, we cannot exclude the possibility of AIRE modulation after a longer period of infection. It is possible that 90 min is a too short time to detect significant increase of AIRE expression, although this event has already been described (Currer et al., 2012; Sun et al., 2014). Even without statistical significance in Aire mRNA expression between HTLV-1-infected and non-infected TEC in our microarray data, we do not exclude a possible post-transcriptional modulation of the corresponding gene expression. This synergy between Aire and NF-κB pathways in TEC, and the enrichment of NF-κB-related biological processes in our global gene expression analysis, may suggest that the constitute activation of NF-κB could enhance Aire expression, and, by consequence, interfere in self-peptide presentation. It also raises the possibility that Tax could modulate the antigen expression by at least two mechanisms: I) avoiding the presentation of virus peptides by MHC, or II) by the expression of viral peptides as self-antigens to thymocytes. The second possibility might explain the weak immune response against HTLV-1.

HTLV-1 establishes a chronic, long lasting infection, and it is intriguing that the host immune system is not quite effective in eliminating this virus infection (Matsuoka and Jeang, 2007). HTLV-1 escapes from immune system surveillance through different mechanisms (Johnson et al., 2001), possibly also including viral reservoirs as additional strategy to avoid an immune response-derived eradication. The thymus could play a major role in this scenario, through TEC HTLV-1 permissiveness and productive infection, and ability to transmit virions to CD4$^+$ T cells as well. In conclusion, our results show that TEC can be infected by cell–cell contact with HTLV-1-infected lymphocytes, and by HTLV-1 cell-free suspensions. In addition, we show here that HTLV-1-infected TEC can attract lymphocytes and convey the virus to CD4$^+$ T cell lines and human primary CD4$^+$ T lymphocytes. This study raises the possibility that TEC play an important role in the pathogenesis of HTLV-1 infection, functioning as viral reservoir and propagator and, thus, eventually contributing to tissue damages in the periphery.

Authors' contributions

LRCB designed and performed experiments, analyzed data wrote the manuscript. LLL designed and performed the microarray assays, cell migration and RT-qPCR experiments, and wrote the manuscript. KMR designed the protocols of cell-free virus infection. NS performed migration assays. MRA participated in design and analysis of microarray and RT-qPCR data, and performed the statistical analysis. MCMM performed and analyzed transmission electron microscopy. DCBH contributed with experimental designs and data interpretation, discussions and manuscript writing. WS conceived the study, coordinated the group and wrote the manuscript. All authors read and approved the final manuscript.

Conflict of interest

The authors declare that they do not have any conflict of interest.

Acknowledgments

This work was funded by the Brazilian research funding agencies CNPq and Faperj, Oswaldo Cruz Foundation (Brazil) and FOCEM (Mercosur). We thank the Hemotherapy Service of the Hospital Clementino Fraga Filho (Federal University of Rio de Janeiro, Brazil) for providing buffy-coats.

Appendix A. Supplementary data

Supplementary data associated with this article can be found, in the online version, at http://dx.doi.org/10.1016/j.imbio.2017.08.001.

References

Andersen, C.L., Ledet-Jensen, J., Orntoft, T., 2004. Normalization of real-time quantitative RT-PCR data: a mode-based variance estimation approach to identify genes suited for normalization, applied to bladder and colon cancer data sets. Cancer Res. 64, 5245–5250.

Ashburner, M., Ball, C.A., Blake, J.A., Botstein, D., Butler, H., Cherry, J.M., Davis, A.P., Dolinski, K., Dwight, S.S., Eppig, J.T., Harris, M.A., Hill, D.P., Issel-Tarver, L., Kasarskis, A., Lewis, S., Matese, J.C., J.E, R., Ringwald, M., Rubin, G.M., Sherlock, G., 2011. The Gene Ontology Consortium. Gene ontology: tool for the unification of biology. Nat. Genet. 25, 25–29. http://dx.doi.org/10.1038/75556.

Benajmini, Y., Hochberg, Y., 1995. Controlling the false discovery rate: a practical and powerful approach to multiple testing author (s): yoav benjamini and yosef hochberg source. J. R. Stati. Soc. Ser. B (Methodol.) 57 (1), 289–300 (Published by: J R Stat. Soc B 57).

Berger, V.W., 2010. Permutation tests for stochastic ordering and ANOVA: theory and applications with r by BASSO, D., PESARIN, F., SALMASO, L., and SOLARI, a. Biometrics 66, 319–321. http://dx.doi.org/10.1007/978-0-387-85956-9.

Carlson, M., 2015. hgug4112a.db: Agilent Human Genome, Whole Annotation Data (chip hgug4112a). R Package Version 3.2.2.hgug4112a.db: Agilent Human Genome, Whole Annotation Data (chip hgug4112a). R Package Version 3.2.2.

Currer, R., Van Duyne, R., Jaworski, E., Guendel, I., Sampey, G., Das, R., Narayanan, A., Kashanchi, F., 2012. HTLV tax: a fascinating multifunctional co-regulator of viral and cellular pathways. Front. Microbiol. 3, 406. http://dx.doi.org/10.3389/fmicb.2012.00406.

Demontis, M.A., Sadiq, M.T., Golz, S., Taylor, G.P., 2015. HTLV-1 viral RNA is detected rarely in plasma of HTLV-1 infected subjects. J. Med. Virol. 87, 2130–2134. http://dx.doi.org/10.1002/jmv.24264.

Derbinski, J., Schulte, A., Kyewski, B., Klein, L., 2001. Promiscuous gene expression in medullary thymic epithelial cells mirrors the peripheral self. Nat. Immunol. 2, 1032–1039. http://dx.doi.org/10.1038/ni723.

Fernández, E., Vicente a Zapata a Brera, B., Lozano, J.J., Martínez, C., Toribio, M.L., 1994. Establishment and characterization of cloned human thymic epithelial cell lines: analysis of adhesion molecule expression and cytokine production. Blood 83, 3245–3254.

Feuer, G., Fraser, J.K., Zack, J.A., Lee, F., Feuer, R., Chen, I.S., Feuer, G., Fraser, J.K., Zack, J.A., Lee, F., Feuer, R., 1996. Human T-cell leukemia virus infection of human hematopoietic progenitor cells: maintenance of virus infection during differentiation in vitro and in vivo. J. Virol. 70, 4038–4044.

Franchini, G., 1995. Molecular mechanisms of human T-cell leukemia/lymphotropic virus type I infection. Blood 86, 3619–3639.

Gentleman, R.C., Carey, V.J., Bates, D.M., Bolstad, B., Dettling, M., Dudoit, S., Ellis, B., Gautier, L., Ge, Y., Gentry, J., Hornik, K., Hothorn, T., Huber, W., Iacus, S., Irizarry, R., Leisch, F., Li, C., Maechler, M., Rossini, A.J., Sawitzki, G., Smith, C., Smyth, G., Tierney, L., Yang, J.Y.H., Zhang, J., 2004. Bioconductor: open software development for computational biology and bioinformatics. Genome Biol. 5http://dx.doi.org/10.1186/gb-2004-5-10-r80. (R-80-80.16).

Ghez, D., Lepelletier, Y., Lambert, S., Fourneau, J.-M., Blot, V., Janvier, S., Arnulf, B., van Endert, P.M., Heveker, N., Pique, C., Hermine, O., 2006. Neuropilin-1 is involved in human T-cell lymphotropic virus type 1 entry. J. Virol. 80, 6844–6854. http://dx.doi.org/10.1128/JVI.02719-05.

Hale, J.S., Fink, P.J., 2009. Back to the thymus: peripheral t cells come home. Immunol. cell Biol. 87, 58–64. http://dx.doi.org/10.1038/icb.2008.87.

Ho, D.D., Rota, T.R., Hirsch, M.S., 1984. Infection of human endothelial cells by human T-lymphotropic virus type I. Proc. Natl. Acad. Sci. U. S. A. 81, 7588–7590.

Hoshino, H., 2012. Cellular factors involved in HTLV-1 entry and pathogenicit. Front. Microbiol. 3, 222. http://dx.doi.org/10.3389/fmicb.2012.00222.

Johnson, J.M., Nicot, C., Fullen, J., Casareto, L., Mulloy, J.C., Jacobson, S., Ciminale, V., Franchini, G., 2001. Free major histocompatibility complex class i heavy chain is preferentially targeted for degradation by human T-cell leukemia/lymphotropic virus type 1 p12 I protein. J. Virol. 75, 6086–6094. http://dx.doi.org/10.1128/JVI.75.13.6086.

Jones, K.S., Petrow-sadowski, C., Bertolette, D.C., Huang, Y., Ruscetti, F.W., 2005. Heparan sulfate proteoglycans mediate attachment and entry of human T-cell leukemia virus type 1 virions into CD4+ T cells. J. Virol. 79, 12692–12702. http://dx.doi.org/10.1128/JVI.79.20.12692.

Jones, K.S., Petrow-Sadowski, C., Huang, Y.K., Bertolette, D.C., Ruscetti, F.W., 2008. Cell-free HTLV-1 infects dendritic cells leading to transmission and transformation of CD4(+) T cells. Nat. Med. 14, 429–436. http://dx.doi.org/10.1038/nm1745.

López-Romero, P., 2011. Pre-processing and differential expression analysis of Agilent microRNA arrays using the AgiMicroRna Bioconductor library. BMC Genom. 12, 64. http://dx.doi.org/10.1186/1471-2164-12-64.

Lepelletier, Y., Smaniotto, S., Hadj-Slimane, R., Villa-verde, D.M.S., Nogueira, A.C., Dardenne, M., Hermine, O., Savino, W., 2007. Control of human thymocyte migration by Neuropilin-1/Semaphorin-3A-mediated interactions. Proc. Natl. Acad. Sci. U. S. A. 104, 5545–5550. http://dx.doi.org/10.1073/pnas.0700705104.

Méndez, E., Kawanishi, T., Clemens, K., Siomi, H., Soldan, S.S., Brady, J., Jacobson, S., Kawanishi, T., Clemens, K., Siomi, H., 1997. Astrocyte-specific expression of human T-cell lymphotropic virus type 1 (HTLV-1) Tax: induction of tumor necrosis factor alpha and susceptibility to lysis by CD8 + HTLV-1-specific cytotoxic T cells. J. Virol. 71, 9143.

Maguer, V., Cassé-Ripoll, H., Gazzolo, L., Dodon, M.D., 1993. Human T-cell leukemia virus type I-induced proliferation of human immature CD2 + CD3- thymocytes. J. Virol. 67, 5529–5537.

Maguer-Satta, V., Gazzolo, L., Dodon, M.D., 1995. Human immature thymocytes as target cells of the leukemogenic activity of human T-cell leukemia virus type I. Blood 86, 1444–1452.

Manca, N., Perandin, F., de Simone, N., Giannini, F., Bonifati, D., Angelini, C., 2002. Detection of HTLV I tax rex and pol gene sequences of thymus gland in a large group of patients with myastenia gravis. J. Acquir. Immune Defic. Syndr. 29, 300–306. http://dx.doi.org/10.1097/00126334-200203010-00012.

Manel, N., Kim, F.J., Kinet, S., Taylor, N., Sitbon, M., Battini, J.-L., 2003. The ubiquitous glucose transporter GLUT-1 is a receptor for HTLV. Cell 115, 449–459.

Matsuoka, M., Jeang, K.-T., 2007. Human T-cell leukaemia virus type 1 (HTLV-1) infectivity and cellular transformation. Nat. Rev. Cancer 7, 270–280. http://dx.doi.org/10.1038/nrc2111.

Moreira-Ramos, K., Castro, F.M.M., De Linhares-Lacerda, L., Savino, W., 2011. Can thymic epithelial cells be infected by human T-lymphotropic virus type 1? Mem. Inst. Oswaldo Cruz 106, 759–762.

Nagai, M., Osame, M., 2003. Human T-cell lymphotropic virus type I and neurological diseases. J. Neurovirol. 9, 228–235. http://dx.doi.org/10.1080/13550280390194028.

Nobrega, C., Roque, S., Nunes-Alves, C., Coelho, A., Medeiros, I., Castro, A.G., Appelberg, R., Correia-Neves, M., 2010. Dissemination of mycobacteria to the thymus renders newly generated T cells tolerant to the invading pathogen. J. Immunol. 184, 351–358. http://dx.doi.org/10.4049/jimmunol.0902152.

Pais-Correia, A.-M., Sachse, M., Guadagnini, S., Robbiati, V., Lasserre, R., Gessain, A., Gout, O., Alcover, A., Thoulouze, M.-I., 2010. Biofilm-like extracellular viral assemblies mediate HTLV-1 cell-to-cell transmission at virological synapses. Nat. Med. 16, 83–89. http://dx.doi.org/10.1038/nm.2065.

Prooyen, N., Van Gold, H., Andresen, V., Schwartz, O., Jones, K., Ruscetti, F., 2010. Human T-cell Leukemia Virus Type 1 p8 Protein Increases Cellular Conduits and Virus Transmission. http://dx.doi.org/10.1073/pnas.1009635107.

R, A., M, D., 2002. A comparison of normalization methods for high density oligonucleotide array data based on variance and bias. Group 19, 1–9.

Ritz, C., Spiess, A.N., 2008. qpcR: An R package for sigmoidal model selection in quantitative real-time polymerase chain reaction analysis. Bioinformatics 24, 1549–1551. http://dx.doi.org/10.1093/bioinformatics/btn227.

Savino, W., 2010. Intrathymic T cell migration is a multivectorial process under a complex neuroendocrine control. Neuroimmunomodulation 17, 142–145. http://dx.doi.org/10.1159/000258708.

Schachtschabel, D., Lazarus, H., Farber, S., Foley, G.E., 1966. Sensitivity os cultured humam lymhoblasts (CCRF-CEM cells) to inhibition by thymidine. Exp. Cell Res. 43, 512–514.

Smith, G.K., 2005. Limma: Linear Models for Microarray Data. Bioinforma. Comput. Biol. Solut. Using R Bioconductor. pp. 397–420.

Starling, A.L.B., Martins-Filho, O.A., Lambertucci, J.R., Labanca, L., de Souza Pereira, S.R., Teixeira-Carvalho, A., Martins, M.L., Ribas, J.G., Carneiro-Proietti, A.B.F., Gonçalves, D.U., 2013. Proviral load and the balance of serum cytokines in HTLV-1-asymptomatic infection and in HTLV-1-associated myelopathy/tropical spastic paraparesis (HAM/TSP). Acta Trop. 125, 75–81. http://dx.doi.org/10.1016/j.actatropica.2012.09.012.

Sun, L., Li, H., Luo, H., Zhao, Y., 2014. Thymic epithelial cell development and its dysfunction in human diseases. Biomed. Res. Int. 2014. http://dx.doi.org/10.1155/2014/206929.

Taylor, G.P., Matsuoka, M., 2005. Natural history of adult T-cell leukemia/lymphoma and approaches to therapy. Oncogene 24, 6047–6057. http://dx.doi.org/10.1038/sj.onc.1208979.

Van Prooyen, N., Andresen, V., Gold, H., Bialuk, I., Pise-Masison, C., Franchini, G., 2010. Hijacking the T-cell communication network by the human T-cell leukemia/lymphoma virus type 1 (HTLV-1) p12 and p8 proteins. Mol. Aspects Med. 31, 333–343. http://dx.doi.org/10.1016/j.mam.2010.07.001.

Vandesompele, J., De Preter, K., Pattyn, F., Poppe, B., Van Roy, N., De Paepe, A., Speleman, F., 2002. Accurate normalization of real-time quantitative RT-PCR data by geometric averaging of multiple internal control genes. Genome Biol. 3http://dx.doi.org/10.1186/gb-2002-3-7-research0034. (Research0034.1).